

Measurement of direct photon production in $p + p$ collisions at $\sqrt{s} = 200$ GeV

S.S. Adler,⁵ S. Afanasiev,²⁰ C. Aidala,¹⁰ N.N. Ajitanand,⁴⁴ Y. Akiba,^{21, 40} A. Al-Jamel,³⁵ J. Alexander,⁴⁴ K. Aoki,²⁵ L. Aphecetche,⁴⁶ R. Armendariz,³⁵ S.H. Aronson,⁵ R. Averbeck,⁴⁵ T.C. Awes,³⁶ V. Babintsev,¹⁷ A. Baldissari,¹¹ K.N. Barish,⁶ P.D. Barnes,²⁸ B. Bassalleck,³⁴ S. Bathe,^{6, 31} S. Batsouli,¹⁰ V. Baublis,³⁹ F. Bauer,⁶ A. Bazilevsky,^{5, 41} S. Belikov,^{19, 17} M.T. Bjorndal,¹⁰ J.G. Boissevain,²⁸ H. Borel,¹¹ M.L. Brooks,²⁸ D.S. Brown,³⁵ N. Bruner,³⁴ D. Bucher,³¹ H. Buesching,^{5, 31} V. Bumazhnov,¹⁷ G. Bunce,^{5, 41} J.M. Burward-Hoy,^{28, 27} S. Butsyk,⁴⁵ X. Camard,⁴⁶ P. Chand,⁴ W.C. Chang,² S. Chernichenko,¹⁷ C.Y. Chi,¹⁰ J. Chiba,²¹ M. Chiu,¹⁰ I.J. Choi,⁵³ R.K. Choudhury,⁴ T. Chujo,⁵ V. Cianciolo,³⁶ Y. Cobigo,¹¹ B.A. Cole,¹⁰ M.P. Comets,³⁷ P. Constantin,¹⁹ M. Csanad,¹³ T. Csorgo,²² J.P. Cussonneau,⁴⁶ D. d'Enterria,¹⁰ K. Das,¹⁴ G. David,⁵ F. Deak,¹³ H. Delagrange,⁴⁶ A. Denisov,¹⁷ A. Deshpande,⁴¹ E.J. Desmond,⁵ A. Devismes,⁴⁵ O. Dietzsch,⁴² J.L. Drachenberg,¹ O. Drapier,²⁶ A. Drees,⁴⁵ A. Durum,¹⁷ D. Dutta,⁴ V. Dzhordzhadze,⁴⁷ Y.V. Efremenko,³⁶ H. En'yo,^{40, 41} B. Espagnon,³⁷ S. Esumi,⁴⁹ D.E. Fields,^{34, 41} C. Finck,⁴⁶ F. Fleuret,²⁶ S.L. Fokin,²⁴ B.D. Fox,⁴¹ Z. Fraenkel,⁵² J.E. Frantz,¹⁰ A. Franz,⁵ A.D. Frawley,¹⁴ Y. Fukao,^{25, 40, 41} S.-Y. Fung,⁶ S. Gadrat,²⁹ M. Germain,⁴⁶ A. Glenn,⁴⁷ M. Gonin,²⁶ J. Gosset,¹¹ Y. Goto,^{40, 41} R. Granier de Cassagnac,²⁶ N. Grau,¹⁹ S.V. Greene,⁵⁰ M. Grosse Perdekamp,^{18, 41} H.-Å. Gustafsson,³⁰ T. Hachiya,¹⁶ J.S. Haggerty,⁵ H. Hamagaki,⁸ A.G. Hansen,²⁸ E.P. Hartouni,²⁷ M. Harvey,⁵ K. Hasuko,⁴⁰ R. Hayano,⁸ X. He,¹⁵ M. Heffner,²⁷ T.K. Hemmick,⁴⁵ J.M. Heuser,⁴⁰ P. Hidas,²² H. Hiejima,¹⁸ J.C. Hill,¹⁹ R. Hobbs,³⁴ W. Holzmann,⁴⁴ K. Homma,¹⁶ B. Hong,²³ A. Hoover,³⁵ T. Horaguchi,^{40, 41, 48} T. Ichihara,^{40, 41} V.V. Ikonnikov,²⁴ K. Imai,^{25, 40} M. Inaba,⁴⁹ M. Inuzuka,⁸ D. Isenhower,¹ L. Isenhower,¹ M. Ishihara,⁴⁰ M. Issah,⁴⁴ A. Isupov,²⁰ B.V. Jacak,⁴⁵ J. Jia,⁴⁵ O. Jinnouchi,^{40, 41} B.M. Johnson,⁵ S.C. Johnson,²⁷ K.S. Joo,³² D. Jouan,³⁷ F. Kajihara,⁸ S. Kametani,^{8, 51} N. Kamihara,^{40, 48} M. Kaneta,⁴¹ J.H. Kang,⁵³ K. Katou,⁵¹ T. Kawabata,⁸ A.V. Kazantsev,²⁴ S. Kelly,^{9, 10} B. Khachaturov,⁵² A. Khanzadeev,³⁹ J. Kikuchi,⁵¹ D.J. Kim,⁵³ E. Kim,⁴³ G.-B. Kim,²⁶ H.J. Kim,⁵³ E. Kinney,⁹ A. Kiss,¹³ E. Kistenev,⁵ A. Kiyomichi,⁴⁰ C. Klein-Boesing,³¹ H. Kobayashi,⁴¹ L. Kochenda,³⁹ V. Kochetkov,¹⁷ R. Kohara,¹⁶ B. Komkov,³⁹ M. Konno,⁴⁹ D. Kotchetkov,⁶ A. Kozlov,⁵² P.J. Kroon,⁵ C.H. Kuberg,^{1, *} G.J. Kunde,²⁸ K. Kurita,⁴⁰ M.J. Kweon,²³ Y. Kwon,⁵³ G.S. Kyle,³⁵ R. Lacey,⁴⁴ J.G. Lajoie,¹⁹ Y. Le Bornec,³⁷ A. Lebedev,^{19, 24} S. Leckey,⁴⁵ D.M. Lee,²⁸ M.J. Leitch,²⁸ M.A.L. Leite,⁴² X.H. Li,⁶ H. Lim,⁴³ A. Litvinenko,²⁰ M.X. Liu,²⁸ C.F. Maguire,⁵⁰ Y.I. Makdisi,⁵ A. Malakhov,²⁰ V.I. Manko,²⁴ Y. Mao,^{38, 40} G. Martinez,⁴⁶ H. Masui,⁴⁹ F. Matathias,⁴⁵ T. Matsumoto,^{8, 51} M.C. McCain,¹ P.L. McGaughey,²⁸ Y. Miake,⁴⁹ T.E. Miller,⁵⁰ A. Milov,⁴⁵ S. Mioduszewski,⁵ G.C. Mishra,¹⁵ J.T. Mitchell,⁵ A.K. Mohanty,⁴ D.P. Morrison,⁵ J.M. Moss,²⁸ D. Mukhopadhyay,⁵² M. Muniruzzaman,⁶ S. Nagamiya,²¹ J.L. Nagle,^{9, 10} T. Nakamura,¹⁶ J. Newby,⁴⁷ A.S. Nyanin,²⁴ J. Nystrand,³⁰ E. O'Brien,⁵ C.A. Ogilvie,¹⁹ H. Ohnishi,⁴⁰ I.D. Ojha,^{3, 50} H. Okada,^{25, 40} K. Okada,^{40, 41} A. Oskarsson,³⁰ I. Otterlund,³⁰ K. Oyama,⁸ K. Ozawa,⁸ D. Pal,⁵² A.P.T. Palounek,²⁸ V. Pantuev,⁴⁵ V. Papavassiliou,³⁵ J. Park,⁴³ W.J. Park,²³ S.F. Pate,³⁵ H. Pei,¹⁹ V. Penev,²⁰ J.-C. Peng,¹⁸ H. Pereira,¹¹ V. Peresedov,²⁰ A. Pierson,³⁴ C. Pinkenburg,⁵ R.P. Pisani,⁵ M.L. Purschke,⁵ A.K. Purwar,⁴⁵ J.M. Qualls,¹ J. Rak,¹⁹ I. Ravinovich,⁵² K.F. Read,^{36, 47} M. Reuter,⁴⁵ K. Reygers,³¹ V. Riabov,³⁹ Y. Riabov,³⁹ G. Roche,²⁹ A. Romana,^{26, *} M. Rosati,¹⁹ S.S.E. Rosendahl,³⁰ P. Rosnet,²⁹ V.L. Rykov,⁴⁰ S.S. Ryu,⁵³ N. Saito,^{25, 40, 41} T. Sakaguchi,^{8, 51} S. Sakai,⁴⁹ V. Samsonov,³⁹ L. Sanfratello,³⁴ R. Santo,³¹ H.D. Sato,^{25, 40} S. Sato,^{5, 49} S. Sawada,²¹ Y. Schutz,⁴⁶ V. Semenov,¹⁷ R. Seto,⁶ T.K. Shea,⁵ I. Shein,¹⁷ T.-A. Shibata,^{40, 48} K. Shigaki,¹⁶ M. Shimomura,⁴⁹ A. Sickles,⁴⁵ C.L. Silva,⁴² D. Silvermyr,²⁸ K.S. Sim,²³ A. Soldatov,¹⁷ R.A. Soltz,²⁷ W.E. Sondheim,²⁸ S.P. Sorensen,⁴⁷ I.V. Sourikova,⁵ F. Staley,¹¹ P.W. Stankus,³⁶ E. Stenlund,³⁰ M. Stepanov,³⁵ A. Ster,²² S.P. Stoll,⁵ T. Sugitate,¹⁶ J.P. Sullivan,²⁸ S. Takagi,⁴⁹ E.M. Takagui,⁴² A. Taketani,^{40, 41} K.H. Tanaka,²¹ Y. Tanaka,³³ K. Tanida,⁴⁰ M.J. Tannenbaum,⁵ A. Taranenko,⁴⁴ P. Tarjan,¹² T.L. Thomas,³⁴ M. Togawa,^{25, 40} J. Tojo,⁴⁰ H. Torii,^{25, 41} R.S. Towell,¹ V.-N. Tram,²⁶ I. Tserruya,⁵² Y. Tsuchimoto,¹⁶ H. Tydesjo,³⁰ N. Tyurin,¹⁷ T.J. Uam,³² J. Velkovska,⁵ M. Velkovsky,⁴⁵ V. Veszpremi,¹² A.A. Vinogradov,²⁴ M.A. Volkov,²⁴ E. Vznuzdaev,³⁹ X.R. Wang,¹⁵ Y. Watanabe,^{40, 41} S.N. White,⁵ N. Willis,³⁷ F.K. Wohn,¹⁹ C.L. Woody,⁵ W. Xie,⁶ A. Yanovich,¹⁷ S. Yokkaichi,^{40, 41} G.R. Young,³⁶ I.E. Yushmanov,²⁴ W.A. Zajc,^{10, †} C. Zhang,¹⁰ S. Zhou,⁷ J. Zimanyi,²² L. Zolin,²⁰ X. Zong,¹⁹ and H.W. vanHecke²⁸

(PHENIX Collaboration)

¹Abilene Christian University, Abilene, TX 79699, USA

²Institute of Physics, Academia Sinica, Taipei 11529, Taiwan

³Department of Physics, Banaras Hindu University, Varanasi 221005, India

⁴Bhabha Atomic Research Centre, Bombay 400 085, India

⁵Brookhaven National Laboratory, Upton, NY 11973-5000, USA
⁶University of California - Riverside, Riverside, CA 92521, USA
⁷China Institute of Atomic Energy (CIAE), Beijing, People's Republic of China
⁸Center for Nuclear Study, Graduate School of Science, University of Tokyo, 7-3-1 Hongo, Bunkyo, Tokyo 113-0033, Japan
⁹University of Colorado, Boulder, CO 80309, USA
¹⁰Columbia University, New York, NY 10027 and Nevis Laboratories, Irvington, NY 10533, USA
¹¹Dapnia, CEA Saclay, F-91191, Gif-sur-Yvette, France
¹²Debrecen University, H-4010 Debrecen, Egyetem tér 1, Hungary
¹³ELTE, Eötvös Loránd University, H - 1117 Budapest, Pázmány P. s. 1/A, Hungary
¹⁴Florida State University, Tallahassee, FL 32306, USA
¹⁵Georgia State University, Atlanta, GA 30303, USA
¹⁶Hiroshima University, Kagamiyama, Higashi-Hiroshima 739-8526, Japan
¹⁷IHEP Protvino, State Research Center of Russian Federation, Institute for High Energy Physics, Protvino, 142281, Russia
¹⁸University of Illinois at Urbana-Champaign, Urbana, IL 61801, USA
¹⁹Iowa State University, Ames, IA 50011, USA
²⁰Joint Institute for Nuclear Research, 141980 Dubna, Moscow Region, Russia
²¹KEK, High Energy Accelerator Research Organization, Tsukuba, Ibaraki 305-0801, Japan
²²KFKI Research Institute for Particle and Nuclear Physics of the Hungarian Academy of Sciences (MTA KFKI RMKI), H-1525 Budapest 114, POBox 49, Budapest, Hungary
²³Korea University, Seoul, 136-701, Korea
²⁴Russian Research Center "Kurchatov Institute", Moscow, Russia
²⁵Kyoto University, Kyoto 606-8502, Japan
²⁶Laboratoire Leprince-Ringuet, Ecole Polytechnique, CNRS-IN2P3, Route de Saclay, F-91128, Palaiseau, France
²⁷Lawrence Livermore National Laboratory, Livermore, CA 94550, USA
²⁸Los Alamos National Laboratory, Los Alamos, NM 87545, USA
²⁹LPC, Université Blaise Pascal, CNRS-IN2P3, Clermont-Fd, 63177 Aubiere Cedex, France
³⁰Department of Physics, Lund University, Box 118, SE-221 00 Lund, Sweden
³¹Institut für Kernphysik, University of Muenster, D-48149 Muenster, Germany
³²Myongji University, Yongin, Kyonggido 449-728, Korea
³³Nagasaki Institute of Applied Science, Nagasaki-shi, Nagasaki 851-0193, Japan
³⁴University of New Mexico, Albuquerque, NM 87131, USA
³⁵New Mexico State University, Las Cruces, NM 88003, USA
³⁶Oak Ridge National Laboratory, Oak Ridge, TN 37831, USA
³⁷IPN-Orsay, Universite Paris Sud, CNRS-IN2P3, BP1, F-91406, Orsay, France
³⁸Peking University, Beijing, People's Republic of China
³⁹PNPI, Petersburg Nuclear Physics Institute, Gatchina, Leningrad region, 188300, Russia
⁴⁰RIKEN (The Institute of Physical and Chemical Research), Wako, Saitama 351-0198, JAPAN
⁴¹RIKEN BNL Research Center, Brookhaven National Laboratory, Upton, NY 11973-5000, USA
⁴²Universidade de São Paulo, Instituto de Física, Caixa Postal 66318, São Paulo CEP05315-970, Brazil
⁴³System Electronics Laboratory, Seoul National University, Seoul, South Korea
⁴⁴Chemistry Department, Stony Brook University, Stony Brook, SUNY, NY 11794-3400, USA
⁴⁵Department of Physics and Astronomy, Stony Brook University, SUNY, Stony Brook, NY 11794, USA
⁴⁶SUBATECH (Ecole des Mines de Nantes, CNRS-IN2P3, Université de Nantes) BP 20722 - 44307, Nantes, France
⁴⁷University of Tennessee, Knoxville, TN 37996, USA
⁴⁸Department of Physics, Tokyo Institute of Technology, Oh-okayama, Meguro, Tokyo 152-8551, Japan
⁴⁹Institute of Physics, University of Tsukuba, Tsukuba, Ibaraki 305, Japan
⁵⁰Vanderbilt University, Nashville, TN 37235, USA
⁵¹Waseda University, Advanced Research Institute for Science and Engineering, 17 Kikui-cho, Shinjuku-ku, Tokyo 162-0044, Japan
⁵²Weizmann Institute, Rehovot 76100, Israel
⁵³Yonsei University, IPAP, Seoul 120-749, Korea

(Dated: December 2, 2024)

Cross sections for midrapidity production of direct photons in $p+p$ collisions at the Relativistic Heavy Ion Collider (RHIC) are reported for transverse momenta of $3 < p_T < 16$ GeV/c. Next-to-leading order (NLO) perturbative QCD (pQCD) describes the data well for $p_T > 5$ GeV/c, where the uncertainties of the measurement and theory are comparable. We also report on the effect of requiring the photons to be isolated from parton jet energy. The observed fraction of isolated photons is well described by pQCD for $p_T > 7$ GeV/c.

PACS numbers: 25.75.Dw

The production of direct photons, i.e. photons not from hadronic decays, in hadron-hadron collisions has been

recognized as providing direct access to the gluon distributions in the hadron, both unpolarized and polarized [1, 2]. The process of direct photon production is described, at high energy and high momentum transfer, by perturbative Quantum Chromodynamics (pQCD). Three parton-parton subprocesses dominate at lowest order: Compton scattering $g + q \rightarrow \gamma + q$; annihilation $q + \bar{q} \rightarrow \gamma + g$; and parton-parton hard scattering with the scattered quark or gluon fragmenting to a photon. Where g (q) represent gluon (quark) states. At next to leading order (NLO), bremsstrahlung emission of photons from the quarks undergoing hard scattering also contributes to the direct photon signal. The annihilation process is suppressed for $p + p$ collisions, due to the lower probability density of \bar{q} versus g in the proton. In general, the fragmentation and bremsstrahlung processes will produce photons in the vicinity of parton jets. Therefore, a requirement that the photon be isolated from parton jet activity can emphasize the Compton graph. Here, only the gluon distribution is unknown, particularly for the polarized case, and direct photon production therefore provides direct access to this (polarized) gluon distribution.

Comparisons of data to theory test our understanding of direct photon production in hadron-hadron collisions. Previous experiments have shown significant disagreement between data and theory at fixed target energy, and good agreement at collider energy [3, 4]. Results from the Relativistic Heavy Ion Collider (RHIC) for $p + p$ collisions cover intermediate energy and momentum transfer, overlapping CERN Intersecting Storage Rings (ISR) and Super antiProton Proton Synchrotron ($Spp\bar{S}$) collider kinematics, and address the robustness of the pQCD prediction for direct photon production. In addition, the comparison of the direct photon rate using no isolation requirement, to the rate of observed photons that are isolated from parton jets, tests our understanding of the processes of parton fragmentation to photons, and of the bremsstrahlung emission of photons from quarks in hard scattering.

Furthermore, direct photon production in $p + p$ collisions provides a valuable baseline for the interpretation of direct photon data from heavy-ion ($A + A$) collisions. Jet-quenching models attribute the strong suppression of high- p_T hadrons in central $A + A$ collisions to energy loss of scattered quarks and gluons in the hot and dense medium created in these collisions [5]. Since photons interact with the medium only electromagnetically, they provide a monitor of the initial parton flux and therefore test a crucial assumption of these models.

In this Letter, we present cross sections for direct photon production in $p + p$ collisions at $\sqrt{s} = 200$ GeV, from the 2003 run of RHIC, at mid-rapidity for $3 < p_T < 16$ GeV/ c . An earlier measurement [6] from the 2002 run of RHIC covered a much smaller region of p_T . Unpolarized cross sections are reported, obtained by averaging

over the spin states of the beams, with $< 1\%$ residual polarization.

The data were collected by the PHENIX detector[7]. The primary detector for this measurement is an electromagnetic calorimeter (EMCal), consisting of two subsystems, a six sector lead-scintillator (PbSc), and a two sector lead glass (PbGl) detector, each located 5 m radially from the beam line. Each sector covers a range of $|\eta| < 0.35$ in pseudo-rapidity and 22.5° in azimuth. The EMCal has fine granularity. Each calorimeter tower covers $\Delta\eta \times \Delta\phi \sim 0.01 \times 0.01$, and a tower contains $\sim 80\%$ of the photon energy hitting the center of the tower. Two photons from $\pi^0 \rightarrow \gamma\gamma$ decays are clearly resolved up to a π^0 p_T of 12 GeV/ c , and a shower profile analysis extends the γ/π^0 discrimination to beyond 20 GeV/ c . The energy calibration of each tower is obtained from minimum-ionizing tracks and from the reconstructed π^0 mass. The uncertainty on the energy scale is less than 1.5%.

Beam-beam counters (BBC) positioned at pseudo-rapidities $3.1 < |\eta| < 3.9$ provide a minimum bias (MB) trigger. Events with high p_T photons are selected by a level-1 trigger that requires a minimum energy deposit of 1.4 GeV in an overlapping tile of 4×4 towers of the EMCal in coincidence with the MB trigger. The MB trigger cross section is $\sigma_{\text{BBC}} = (23.0 \pm 2.2)$ mb, about 50% of $\sigma_{\text{inel}}^{pp}$. The efficiency bias due to the MB trigger in the 2003 run, $\epsilon_{\text{bias}} = 0.79 \pm 0.02$, is determined from the ratio of the yield of high $p_T \pi^0$ with and without the MB trigger. An integrated luminosity (\mathcal{L}) of 240 nb $^{-1}$ after a vertex cut of ± 30 cm is used in this analysis.

The first step in the analysis is to cluster the hit towers. If there are two tower energy maxima and at least one lower-energy tower between them, the cluster is split into two, with the energy of each tower divided between the two clusters according to electromagnetic shower profiles associated with the clusters. Photons are identified by a shower profile cut that was calibrated using test beam data, identified electrons, and decay photons from identified π^0 . The cut rejects $\sim 50\%$ of hadrons depositing $E > 3$ GeV in the EMCal and accepts $\sim 98\%$ of real photons. The charged particle veto of the photon sample is based on tracks in drift chambers 2 m from the beamline, and hits in the pad chamber (PC3) immediately in front of the EMCal. Loss of photons from conversions in material before the EMCal is estimated using a GEANT [8] simulation and confirmed by the observed fraction of identified π^0 photons vetoed. The conversion correction is 3% for the drift chamber veto and $\sim 8\%$ for the PC3 veto. Remaining non-photon background, including converting neutral hadrons and albedo from the magnet yokes, is also estimated from the GEANT simulation at $\sim 1\%$.

The experimental challenge in direct-photon measurements is the large photon background from decays of hadrons, primarily from $\pi^0 \rightarrow \gamma\gamma$ ($\sim 80\%$ of the decays)

and $\eta \rightarrow \gamma\gamma$ ($\sim 15\%$). We use two techniques described below to subtract the decay background: a π^0 tagging method and a cocktail subtraction method.

In the π^0 tagging method, a candidate photon is tagged as a π^0 decay photon if it forms a pair with another photon in the mass range $105 < M_{\gamma\gamma} < 165$ MeV ($M_{\pi^0} \pm 3\sigma$), with $E_\gamma > 150$ MeV. A fiducial region for direct photon candidates excludes 10 towers (0.1 radians) from the edges of the EMCAL, while partner photons are accepted over the entire detector, to improve the probability of observing both decay photons from the π^0 .

This method overestimates the yield of photons from π^0 decays, γ_{π^0} , due to combinatorial background. A p_T dependent correction ($\sim 10\%$) is estimated from a fit to the π^0 sidebands, with $\pm 3\%$ uncertainty. The yield of direct photons, γ_{dir} , is obtained from the inclusive photon yield, γ_{incl} , using the equation

$$\gamma_{\text{dir}} = \gamma_{\text{incl}} - (1 + \delta_{h/\pi^0}^\gamma)(1 + R_{\pi^0}^{\text{miss}})\gamma_{\pi^0}, \quad (1)$$

where $R_{\pi^0}^{\text{miss}}$ is the correction for missing photon partners to the π^0 ; $(1 + R_{\pi^0}^{\text{miss}})\gamma_{\pi^0}$ represents the total contribution of photons from π^0 decays in each p_T^γ bin and δ_{h/π^0}^γ is the fraction of photons from hadrons other than π^0 .

To estimate $R_{\pi^0}^{\text{miss}}$, a Monte Carlo simulation is used that includes the acceptance, energy resolution and our measured π^0 spectrum [9] as input. Figure 1 shows $(1 + R_{\pi^0}^{\text{miss}})$ from the simulation. The largest uncertainty is from the calibration of the EMCAL at low energy. δ_{h/π^0}^γ is estimated by a simulation of hadron decays based on the η/π^0 [10] and ω/π^0 [11] ratios from our measurements: $\delta_{h/\pi^0}^\gamma \approx 0.24$ with $\delta_{\eta/\pi^0}^\gamma = 0.19$ and $\delta_{\omega/\pi^0}^\gamma = 0.05$. The contribution from other hadrons is less than 0.01. A small p_T dependence is assumed to follow m_T scaling [12]. The inset of Fig.1 shows the fraction of photons from h , π^0 and γ_{dir} to γ_{incl} . The direct photon fraction ranges from 10% at low p_T^γ to 50% for $p_T^\gamma > 10$ GeV.

In the cocktail method [6, 13], the spectrum of decay photons is simulated utilizing our measured π^0 spectrum and applying m_T scaling in order to account for other hadronic contributions. The effect of shower merging is also taken into account in the simulation. A double ratio $R_\gamma = (\gamma/\pi^0)^{\text{data}} / (\gamma/\pi^0)^{\text{sim}}$, is calculated for each p_T bin. $R_\gamma > 1$ indicates a direct photon signal. The direct photon yield is extracted as $\gamma_{\text{dir}} = (1 - R_\gamma^{-1}) \cdot \gamma_{\text{incl}}$. Using the γ/π^0 ratio has the advantage that some systematic uncertainties cancel.

A summary of the systematic uncertainties is presented in Table I. Uncertainties of similar contributions are grouped together: global quantities (a), the inclusive photon yield (b) and the direct photon background (c-e). The categories (a)-(d) apply to both analysis methods. Category (a) includes the uncertainties of the energy scale, luminosity, and geometrical acceptance. The main contribution to category (b) is the uncertainty of the non-photon background estimation. The uncertainty of the

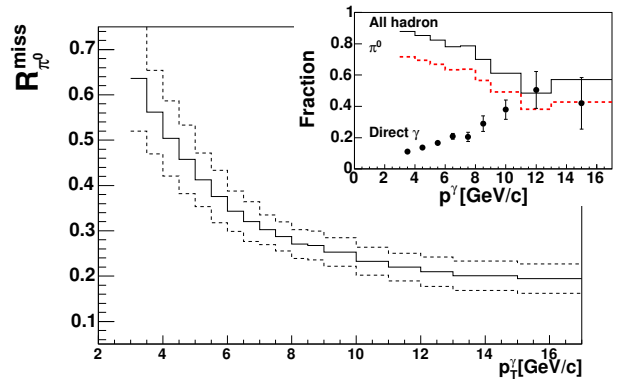


FIG. 1: Correction for missing photon partners to the π^0 ($R_{\pi^0}^{\text{miss}}$) vs. p_T^γ . Dashed lines show the systematic uncertainty. Inset: Different contributions to the inclusive photon spectrum. Solid (dashed) lines represent all hadronic (π^0) decay contributions. The data points show the remaining photon contributions.

charged particle veto is based on a study of the cluster vs. track matching in the EMCAL and the tracking detectors. The uncertainty in the neutral hadron contamination is estimated from identified charged hadrons. We assign the estimate of the albedo contribution as its uncertainty. Category (c) includes uncertainties of the correction for combinatorial background as estimated by different parameterizations of the background shape and the uncertainties of the π^0 reconstruction efficiency. Category (d) refers to the uncertainty of contributions from hadronic decays other than π^0 's, derived from our measurement of the hadron production ratios. Finally, category (e) combines all remaining uncertainties separately for the two analysis methods. Non-linearity effects in the energy calibration affect the minimum energy cut in the π^0 tagging method (e₁) and distort the π^0 spectra in the cocktail method (e₂). After the individual calibration a difference in the γ/π^0 ratio of PbGl and PbSc remains (5–7%). This is used to assign a systematic uncertainty of the non-linear part of the energy scale. Due to the small signal fraction at low p_T , this translates into the large relative uncertainty in the direct photon spectra in Table I. In addition the uncertainty of the shower profile analysis of the γ/π^0 discrimination at high p_T is included in this category. The two uncertainties (e₁,e₂) are combined by averaging the squared uncertainties, and then all uncertainties were added in quadrature.

The results from the tagging and cocktail methods, obtained from independent analyses, agree within systematic uncertainties. We report an average of the results, and uncertainties, of the two methods giving equal weight to the two analysis methods. average of the results, and uncertainties, of the approach gives equal weight to the two analysis methods.

The invariant cross section of direct photon production

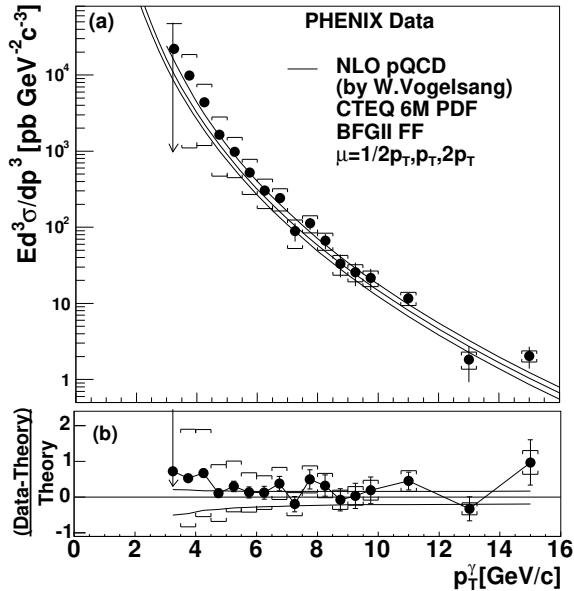


FIG. 2: (a) Direct photon spectra with NLO pQCD calculations for three theory scales, μ . Brackets around data points show systematic errors. (b) Comparison to the NLO pQCD calculation for $\mu = p_T$, with upper and lower curves for $\mu = p_T/2$ and $2p_T$.

is calculated by the following formula,

$$E \frac{d^3\sigma}{dp_T^3} = \frac{1}{\mathcal{L}} \frac{1}{2\pi p_T} \frac{\gamma_{\text{dir}}}{\Delta p_T \Delta y} \frac{1}{\epsilon} \frac{1}{\epsilon_{\text{bias}}}, \quad (2)$$

where ϵ includes geometrical acceptance and the smearing effect from the energy resolution. The data points are plotted at the bin centers, with a correction to take into account the effect of finite bin sizes. The uncertainty of this correction is small compared to other systematic uncertainties.

Figure 2 shows the measured invariant cross section for mid-rapidity direct photon production at $\sqrt{s} = 200$ GeV.

TABLE I: Relative systematic uncertainties of the direct photon spectra.

p_T [GeV/c]	4.5-5	7.5-8	10-12
Signal fraction	9%	27%	49%
(a) Global	16.8%	14.9%	14.9%
(b) Inclusive photons	12.3%	4.7%	3.1%
(c) Photons from π^0	30.1%	10.7%	6.5%
(d) Other hadrons	21.4%	6.7%	3.8%
(e) Non-linearity (+ remaining)			
(e ₁) π^0 tagging	42.7%	6.8%	5.4%
(e ₂) cocktail	69.5%	20.4%	13.4%
Total	71.6%	25.2%	19.8%

In addition, a NLO pQCD prediction [14, 15, 16, 17, 18, 19], using CTEQ 6M parton distribution functions [20] and the BFG II parton to photon fragmentation function [21], is shown with three theory scales (μ) as indicated. The bottom panel shows the fractional difference between the data and this calculation. The results are well described by pQCD.

The direct photon sample includes photons from the Compton and annihilation subprocesses, which are expected to be isolated from parton jet activity. To measure the fraction of isolated photons, we apply an isolation requirement in the π^0 tagging analysis method. Isolated photons are selected with less than 10% additional energy within a cone of radius $\Delta r = \sqrt{(\Delta\eta)^2 + (\Delta\phi)^2} = 0.5$ around the candidate photon direction. The cone energy is the sum of track momenta in the drift chamber and EMC energy. In most cases the cone is larger than the PHENIX acceptance and this is corrected for with a 0.08 increase in the photon isolation fraction in the theory predictions below [22].

Figure 3 presents the results of the isolation cut for photons from the π^0 tagging method. Closed circles show the fraction of isolated direct photons to all direct photons. The curves are predictions from NLO pQCD, for the parton distribution and fragmentation functions as in Fig. 2, and for an additional parton to photon fragmentation function. The observed ratio is $\sim 90\%$ for $p_T^\gamma > 7$ GeV/c and it is well described by pQCD. An additional loss of $\sim 15\%$ ($p_T^\gamma = 3$ GeV/c) to less than 5% (for $p_T^\gamma > 10$ GeV/c) due to the underlying event is estimated by a PYTHIA[23] simulation. Finally, for comparison, the open circles show the ratio of isolated photons from π^0 decays to all photons from π^0 decays. This indicates significantly less isolation than in the direct photon sample.

In summary, invariant cross sections for direct photon production at mid-rapidity have been measured up to $p_T = 16$ GeV/c in $\sqrt{s} = 200$ GeV $p + p$ collisions. The data are well described by NLO pQCD predictions for $p_T > 5$ GeV/c where the uncertainties of the measurement and theory are comparable. When these data are combined with fixed target and Tevatron collider data, these measurements demonstrate the robustness of the pQCD description of direct photon production [25]. In addition, the ratio of isolated photons to all non-hadronic decay photons is well-described by pQCD for $p_T > 7$ GeV/c.

Based on the comparison of high p_T direct photon data from $Au + Au$ collisions at RHIC with a $p + p$ reference from NLO pQCD, the origin of the observed suppression of high- p_T hadrons in central $Au + Au$ collisions can be attributed to properties of the hot and dense matter created in the $Au + Au$ collision [13]. The measurements presented here confirm this conclusion and put it on a firm experimental basis. Furthermore, the successful description of direct photon production at RHIC is a nec-

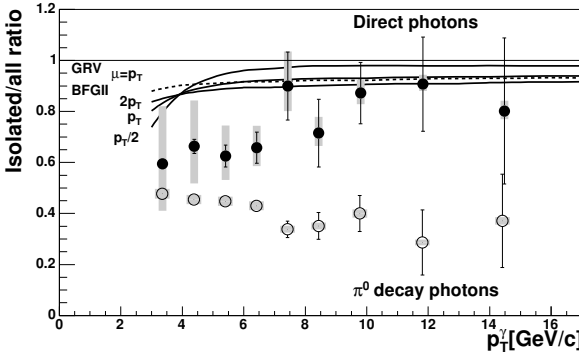


FIG. 3: Closed circles: Ratio of isolated direct photons to all direct photons from the π^0 -tagging method. The statistical uncertainties are shown as black error bars and the systematic uncertainties are plotted as shaded bars. The solid and dashed curves are NLO pQCD calculations with three theory scales for BFGII [21] and one scale for GRV [24] parton to photon fragmentation functions. Open circles: Ratio of isolated photons from π^0 decays to all photons from π^0 decays.

essary test for the extraction of the gluon polarization from direct photon production in collisions of longitudinally polarized protons.

We thank the staff of the Collider-Accelerator and Physics Departments at BNL for their vital contributions. We thank Michel Fontannaz, Werner Vogelsang, and Monique Werlen for their interest and input. We acknowledge support from the Department of Energy and NSF (U.S.A.), MEXT and JSPS (Japan), CNPq and FAPESP (Brazil), NSFC (China), IN2P3/CNRS, CEA, and ARMINES (France), BMBF, DAAD, and AvH (Germany), OTKA (Hungary), DAE and DST (India), ISF (Israel), KRF and CHEP (Korea), RMIST, RAS, and RMAE (Russia), VR and KAW (Sweden), U.S. CRDF

for the FSU, US-Hungarian NSF-OTKA-MTA, and US-Israel BSF.

* Deceased

† PHENIX Spokesperson: zajc@nevis.columbia.edu

- [1] C. Papavassiliou et al., Phys. Rev. D **26**, 3284 (1982).
- [2] E. L. Berger and J. W. Qiu, Phys. Rev. D **40**, 3128 (1989).
- [3] W. Vogelsang and M. R. Whalley, J. Phys. G **23**, 1 (1997).
- [4] P. Aurenche et al., Eur. Phys. J. **C9**, 107 (1999).
- [5] K. Adcox et al., Nucl. Phys. A **757**, 184 (2005).
- [6] S. S. Adler et al., Phys. Rev. D **71**, 071102 (2005).
- [7] K. Adcox et al., Nucl. Instrum. Meth. **A499**, 469 (2003).
- [8] *GEANT 3.2.1 Manual* (1994), CERN W5013, URL <http://wwwasdoc.web.cern.ch/wwwasdoc/pdfdir/geant.pdf>.
- [9] S. S. Adler et al., Phys. Rev. Lett. **91**, 241803 (2003).
- [10] S. S. Adler et al., Phys. Rev. Lett. **96**, 202301 (2006).
- [11] V. Ryabov et al. (2005), hep-ex/0510017.
- [12] K. Adcox et al., Phys. Rev. Lett. **88**, 192303 (2002).
- [13] S. S. Adler et al., Phys. Rev. Lett. **94**, 232301 (2005).
- [14] L. E. Gordon and W. Vogelsang, Phys. Rev. D **48**, 3136 (1993).
- [15] L. E. Gordon and W. Vogelsang, Phys. Rev. D **50**, 1901 (1994).
- [16] P. Aurenche et al., Phys. Lett. B **140**, 87 (1984).
- [17] P. Aurenche et al., Nucl. Phys. B **297**, 661 (1988).
- [18] H. Baer et al., Phys. Rev. D **42**, 61 (1990).
- [19] H. Baer et al., Phys. Lett. B **234**, 127 (1990).
- [20] J. Pumplin et al., JHEP **0207**, 012 (2002).
- [21] L. Bourhis et al., Eur. Phys. J. **C2**, 529 (1998).
- [22] W. Vogelsang, private communication.
- [23] T. Sjöstrand et al. (2003), (Rick Field's Tune A has been used), hep-ph/0308153.
- [24] M. Gluck et al., Phys. Rev. D **51**, 1427 (1995).
- [25] P. Aurenche et al., Phys. Rev. D **73**, 94007 (2006).